

# Constraints on Jupiter's Hydrogen Corona from Galileo UVS Observations

G.R. Gladstone<sup>a,\*</sup> W.R. Pryor<sup>b</sup> W.K. Tobiska<sup>c</sup>  
A.I.F. Stewart<sup>d</sup> K.E. Simmons<sup>d</sup> J.M. Ajello<sup>e</sup>

<sup>a</sup>*Southwest Research Institute, San Antonio, TX, USA*

<sup>b</sup>*Hampton University, Hampton, VA, USA*

<sup>c</sup>*Space Environment Technologies, Pacific Palisades, CA, USA*

<sup>d</sup>*Laboratory for Atmospheric and Space Physics, University of Colorado, Boulder, CO, USA*

<sup>e</sup>*Jet Propulsion Laboratory, California Institute of Technology, Pasadena, CA, USA*

---

## Abstract

During Galileo orbits C10 and E11, the Ultraviolet Spectrometer (UVS) obtained H Ly $\alpha$  scans at low latitudes across the disk of Jupiter from a phase angle of 90°–109° and a distance of 18–21 jovian radii. Jupiter's nightside Lyman alpha brightness was about 0.5 kR, approximately half as bright as interplanetary space. From the nightside to the dayside, the Lyman alpha brightness rose to a peak of  $\sim 15$  kR near the sub-solar limb and then dropped sharply to interplanetary brightness levels. On orbit C10 three disk scans were obtained (near 30°N latitude, 21°S latitude, and along the equator), while a single equatorial scan was made on orbit E11. The steep falloff in Ly $\alpha$  brightness at the sub-solar point provides a strong constraint on the distribution of atomic hydrogen in the upper atmosphere. All disk scans are reasonably well fit by a resonance line radiative transfer code which assumes a total H column density of  $6 \times 10^{16} \text{ cm}^{-2}$  above the methane homopause at 340 km, and a temperature profile consistent with the Galileo Probe results with an exospheric temperature of 940 K. However, we find that the inclusion of a small amount of "hot" hydrogen, with an abundance described by a Chapman profile, can substantially improve the fit to the UVS limb scan data. Just such a hot hydrogen component is expected in the upper atmosphere of Jupiter, and has been previously invoked to explain observations of the jovian Ly $\alpha$  line profile made from Earth orbit. The best fit to the UVS data occur with a hot H column density that is 0.1% of the ambient H column, with an effective temperature of 25,000 K and a topside scale height of 1000 km (in our empirical representation, the hot H scale height is unrelated to the hot H temperature). Other combinations of column abundance and effective temperature can also provide good fits to the data. As long as the hot H is located above the homopause, there is no strong dependence on the height of the Chapman profile.

## 1 Introduction

The Voyager missions found remarkably hot upper atmospheres on all the giant planets, far in excess of predictions based on solar EUV driven processes, with thermospheric temperatures of 1000 K or more. (e.g., Gladstone et al., 2002). The heating mechanism is still debated, but may involve 1) transported heat from energetic particle and Joule heating in the auroral regions, 2) soft particle precipitation at low latitudes, and 3) gravity wave deposition of energy (either locally or from waves generated in the auroral regions). The Galileo mission to Jupiter provided an opportunity to measure H limb profiles from close range, to see if an escaping or almost escaping “hot H” component was present, as has been suggested to explain line profile data obtained with International Ultraviolet Explorer (IUE) (Ben Jaffel et al., 1993) and Hubble Space Telescope (HST) (Emerich et al., 1996). The Galileo UVS (Hord et al., 1992) was used in a 16-wavelength “miniscan” mode to make scans of Jupiter’s Ly $\alpha$  dayglow emissions from above the dawn terminator (on Sept. 17, 1997) and the dusk terminator (on Nov. 8, 1997), during orbits C10 and E11, respectively. Here we present the UVS data from these scans, and model the observed Ly $\alpha$  dayglow to search for the presence of hot H.

## 2 Data

During these measurements the UVS grating drive would 1) scan for 4 s over the wavelength range from 110.51–123.98 nm, 2) stop taking data for 1/3 s, 3) scan for 4 s over the wavelength range from 117.34–130.74 nm, 4) stop for another 1/3 s, and 5) repeat the cycle. During each 4 s period, 528 grating steps of 0.15 nm were used to scan each 88-step spectral region 6 times. The spectral resolution was  $\sim 0.7$  nm, suitable for isolating Ly $\alpha$  from the surrounding H<sub>2</sub> band emissions. Grating steps not on the Ly $\alpha$  line were used to estimate the combined background from energetic particles and H<sub>2</sub> band count rates. The background-subtracted Ly $\alpha$  brightnesses for the C10 and E11 orbits are shown in Figs. 1 and 2, plotted as 1 point per 4.33 s. The observing geometry for each slew across Jupiter is described in Table 1. The ‘Drift’ column gives the slit

---

\* Corresponding author.

*Email address:* rgladstone@swri.edu (G.R. Gladstone).

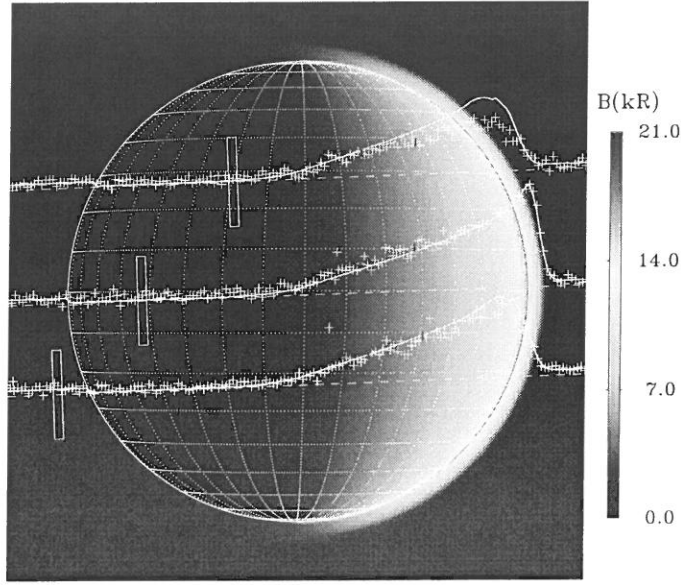


Fig. 1. Disk scans of  $\text{Ly}\alpha$  dayglow brightness across Jupiter obtained by the Galileo UVS on Sept. 17, 1997 (during the C10 orbit) are shown on a simulated  $\text{Ly}\alpha$  image. The data are shown by crosses and the nominal model fit by solid lines; the track of the UVS slit and its footprint are also shown. The red vertical bars on each scan show  $1\text{-}\sigma$  error bars. The color bar provides the model brightness in kR.

Table 1  
Observing geometry for Galileo UVS  $\text{Ly}\alpha$  disk scans.

Orbit	Day of 1997	UT	Phase ( $^{\circ}$ )	Lat ( $^{\circ}$ )	Long ( $^{\circ}$ )	Range ( $10^6$ km)	Slit Width (km)	Drift (km)
C10	260	12:33:26-13:38:09	95.56	29.64	333.97	1.508	2631	908
			95.47	-21.16	347.51	1.494	2607	911
			95.33	0.74	356.67	1.486	2593	997
E11	312	03:56:34-04:28:55	109.26	12.75	259.01	1.290	2251	1039

footprint motion during each 4 s integration period. During each scan the UVS slowly slewed from off the dark limb to off the bright limb of Jupiter, with the  $0.1^{\circ} \times 1.0^{\circ}$  slit aligned approximately north-south, with slowly varying latitude. For the C10 observations three scans were made, at latitudes of about  $30^{\circ}\text{N}$ ,  $21^{\circ}\text{S}$ , and along the equator, while the E11 observation was a single equatorial scan.

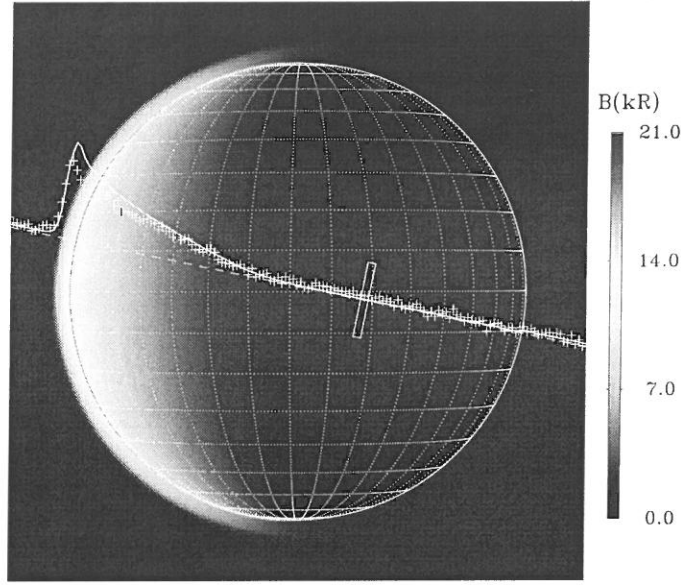


Fig. 2. Same as for Fig. 1, except for the data taken on Nov. 8, 1997 (during the E11 orbit). On this orbit only one disk scan was made.

### 3 Model

We use an equatorial model atmosphere based on the standard NEB model atmosphere of Gladstone et al. (1996) scaled to a double-sided Bates fit to the pressure-temperature profile of Seiff et al. (1998), as shown in Fig. 3. The resonance line radiative transfer of dayglow  $\text{Ly}\alpha$  is calculated for several solar zenith angles using the 1-D REDISTER model described by Gladstone (1988). Solar  $\text{Ly}\alpha$  fluxes ( $3.75 \times 10^{11}$  and  $3.93 \times 10^{11}$  ph/cm<sup>2</sup>/s at 1 AU for the C10 and E11 observations, respectively) are taken from UARS/SOLSTICE and adjusted for the different solar longitudes of Earth and Jupiter. The final source function and the extinction are interpolated onto the line-of-sight for each pixel of the simulated images shown in Figs. 1 and 2, and the brightness calculated by formal solution of the radiative transfer equation.

The interstellar medium (ISM)  $\text{Ly}\alpha$  background for the viewing geometries of Figs. 1 and 2 were estimated to be 800 R and 425 R, respectively, using the code of Pryor et al. (2001), and these values are in good agreement with the observations. The ISM  $\text{Ly}\alpha$  emission scattered by Jupiter, which is expected to dominate the nightside brightness, was not precisely calculated for this work. Instead, we have included the reflected ISM emissions as a uniform 120 R over the planet, based on a typical nightside hemisphere ISM brightness of

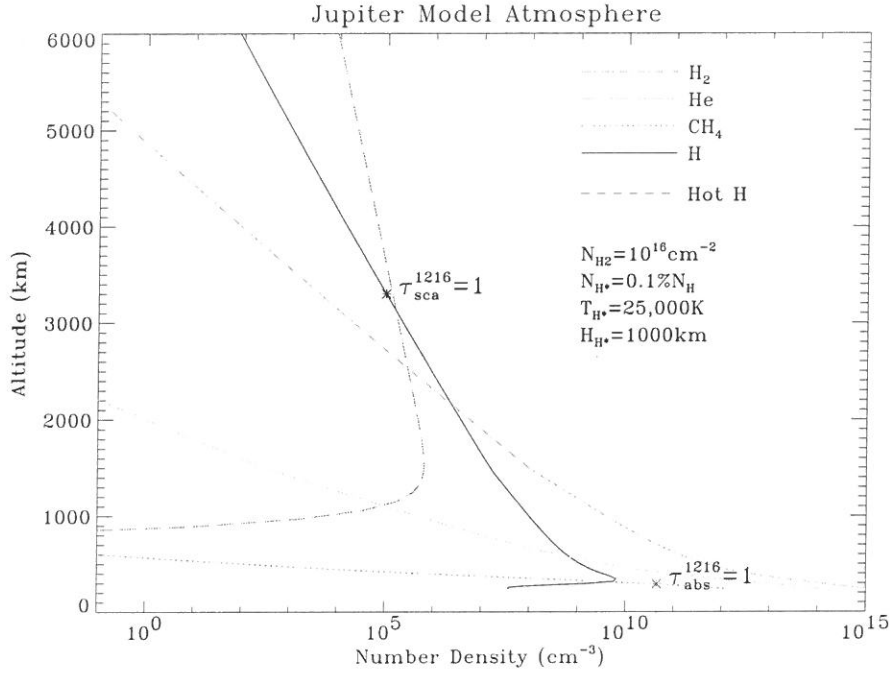


Fig. 3. Model atmosphere for the equatorial region of Jupiter. The densities of H, H<sub>2</sub>, He, and CH<sub>4</sub> from the NEB model of Gladstone et al. (1996) have been scaled to a double-sided Bates fit to the P-T profile determined by Seiff et al. (1998) from Galileo probe data. The nominal hot H profile is shown, with parameters as listed, and the unit optical depths for Ly $\alpha$  absorption by CH<sub>4</sub> and line-center scattering by H are also indicated. The line-center scattering optical depth is  $\sim 30,000$  at the altitude of unit absorption optical depth.

$\sim 600$  R, and an atmosphere Ly $\alpha$  reflectivity of  $\sim 20\%$  (based on model simulations). The observed nightside brightness is  $\sim 500$  R, so that low-latitude particle precipitation may make a substantial contribution, as earlier deduced by McConnell et al. (1980) using Voyager Ultraviolet Spectrometer (UVS) data. However, a more rigorous calculation of the scattered ISM Ly $\alpha$  needs to be done to confirm this result.

Based on the modeling of auroral hot H by Bisikalo et al. (1996), we attempt to improve the model fit to the data by including an empirical hot H distribution in the form of a Chapman profile. Hot H is expected to be produced in the upper atmosphere of Jupiter through a variety of processes, some of which are listed in Table 2.

The hot H is described by four parameters, 1) the level of peak hot H density, which we describe by  $N_{H_2}$ , the column density of ambient H<sub>2</sub> at that level, 2)

Table 2

Example reactions for producing hot H.

---

$\text{H}_2(v > 0) + \text{H}$	$\rightarrow$	$\text{H}_2(v' < v) + \text{H}^*$
$\text{H}_2 + \text{H}_2^+$	$\rightarrow$	$\text{H}_3^+ + \text{H}^*$
$\text{e} + \text{H}_3^+$	$\rightarrow$	$\text{H}_2 + \text{H}^*$
	$\rightarrow$	$3 \text{H}^*$
$\text{e}^* + \text{H}_2$	$\rightarrow$	$\text{H}_2^* + \text{e}^* \rightarrow 2 \text{H}^* + \text{e}^*$

---

the column of hot H,  $N_{\text{H}^*}$ , which is given as a percentage of the ambient H column of  $9.0 \times 10^{16} \text{ cm}^{-2}$ , 3) the hot H scale height,  $H_{\text{H}^*}$ , and 4) the hot H temperature,  $T_{\text{H}^*}$ , which we take as 25,000 K and which is independent of the hot H scale height. Using the nominal values for these parameters given in Fig. 3, we obtain the simulated images shown in Figs. 1 and 2. Integrating the simulated images over the slit at each location during the scans yields the fits to the UVS data shown.

## 4 Results

The nominal hot H model provides a very reasonable fit to the observed UVS Ly $\alpha$  dayglow brightnesses across the disk and past the limb. In contrast with the Voyager UVS observations of equatorial Ly $\alpha$  investigated by McConnell et al. (1980), we find no evidence of an unusually slow decrease in brightness across the terminator, even using 1-D radiative transfer calculations. This discrepancy could result from many possible sources (e.g., different instruments, different epochs, different models) and will not be addressed further. Instead, we wish to further investigate whether the Galileo UVS data can provide constraints on the presence of hot H in Jupiter’s upper atmosphere.

To test the sensitivity of the results to the assumed hot H profile, we varied the parameters of the Chapman function and recalculated the model brightnesses. These results are presented in 1) Figs. 4 and 5 for variation of the level of peak hot H density, 2) Figs. 6 and 7 for variation of the total hot H column density, Figs. 8 and 9 for variation of the hot H scale height, and Fig. 10 for variation of the assumed hot H effective temperature. While varying the level of peak hot H density had little effect, the magnitudes of the brightnesses are very sensitive to the total column of hot H, while the shapes of the brightness profiles are very sensitive to the hot H scale height. Note that the results for no hot H at all, as shown by the  $N_{\text{H}^*} = 0\%$  curves in Fig. 7, do not provide nearly as good a fit to the data as the nominal hot H model. Thus, these UVS data support the idea of a modest hot H corona on Jupiter, although our results would be improved with the use of a physically-based rather than

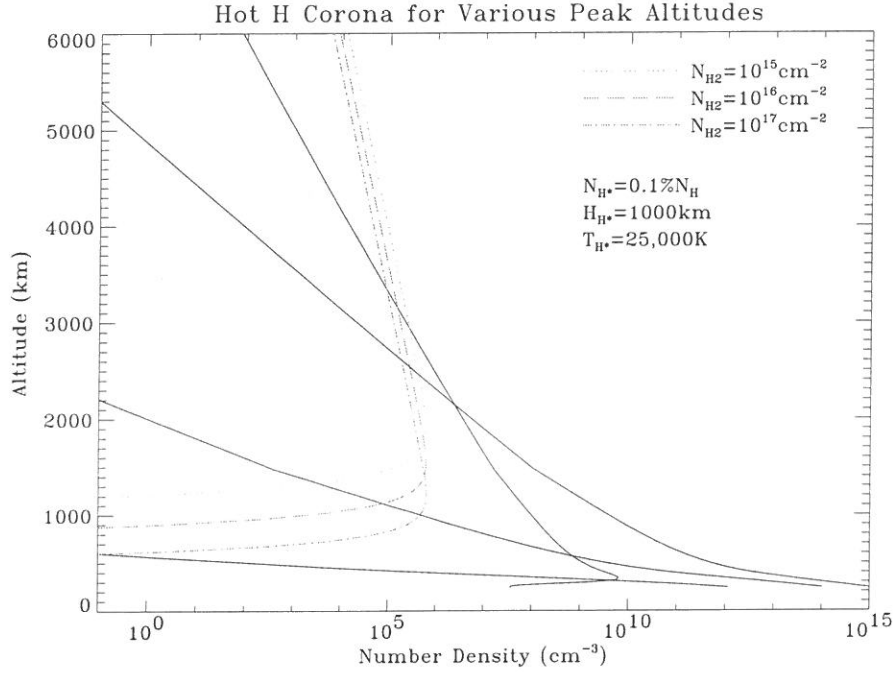


Fig. 4. Hot H profiles used for a study of the sensitivity of the model to variations in the level of peak hot H density. The remaining hot H parameters are held at their nominal values.

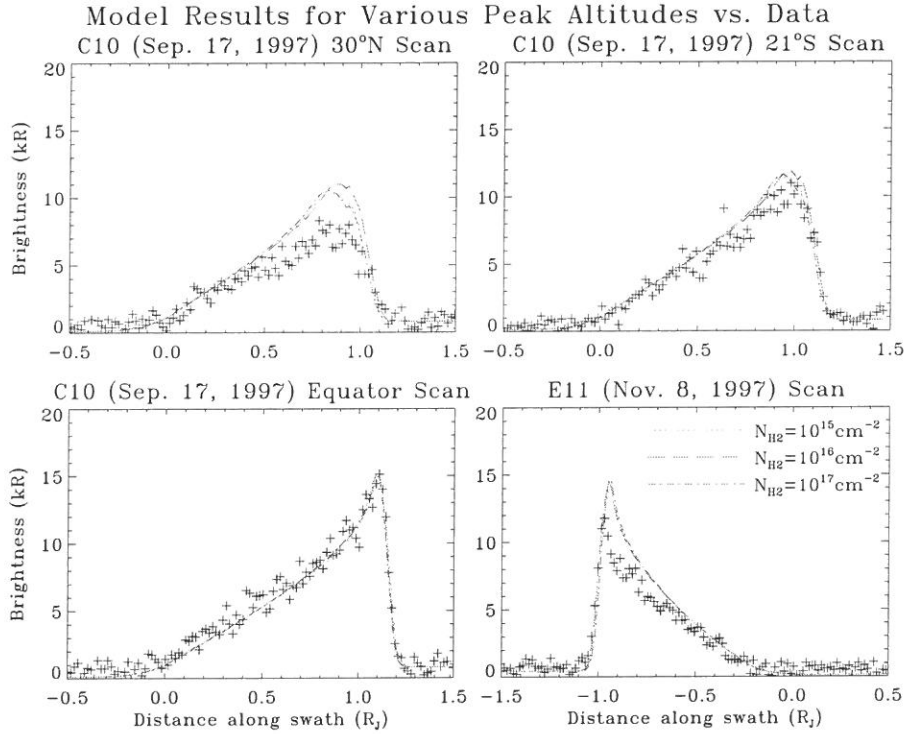


Fig. 5. The results of varying the level of peak hot H density on the model brightnesses. No strong dependence is seen for a factor of 10 increase or decrease in  $N_{H2}$ .

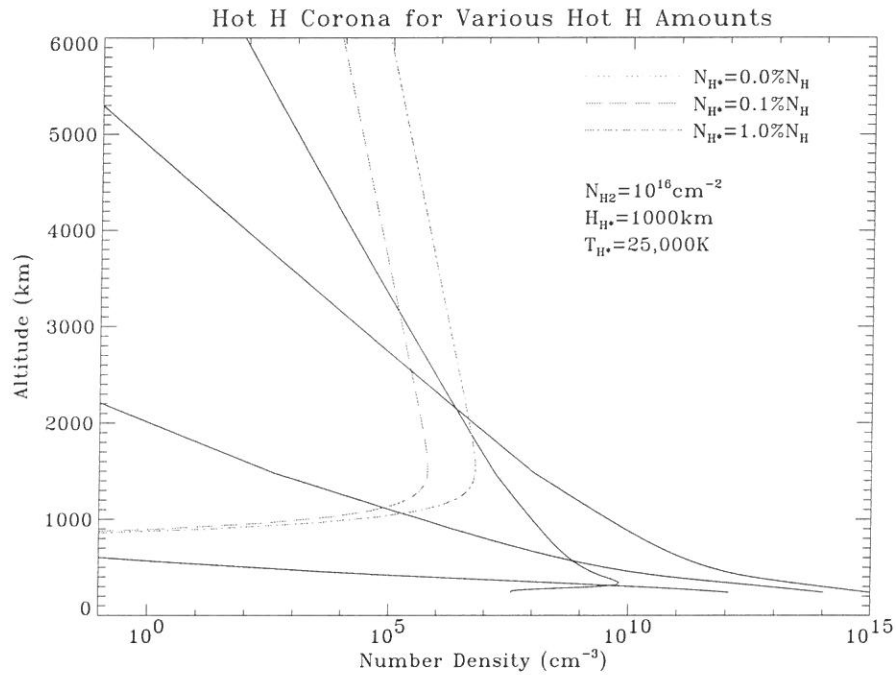


Fig. 6. Hot H profiles used for a study of the sensitivity of the model to variations in the hot H column density. The remaining hot H parameters are held at their nominal values.

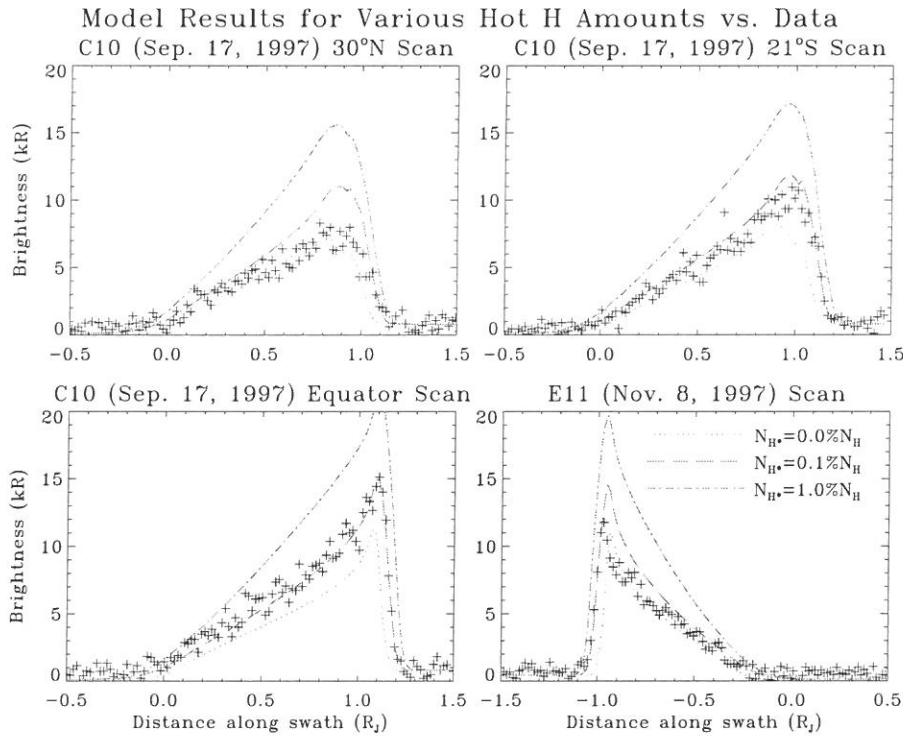


Fig. 7. The results of varying the hot H column density on the model brightnesses. The model brightness is very sensitive to the hot H column density, and  $N_{H*}=0.1\%N_H$  provides a substantially better fit to the data than either no hot H at all or as much as  $1.0\%N_H$ .



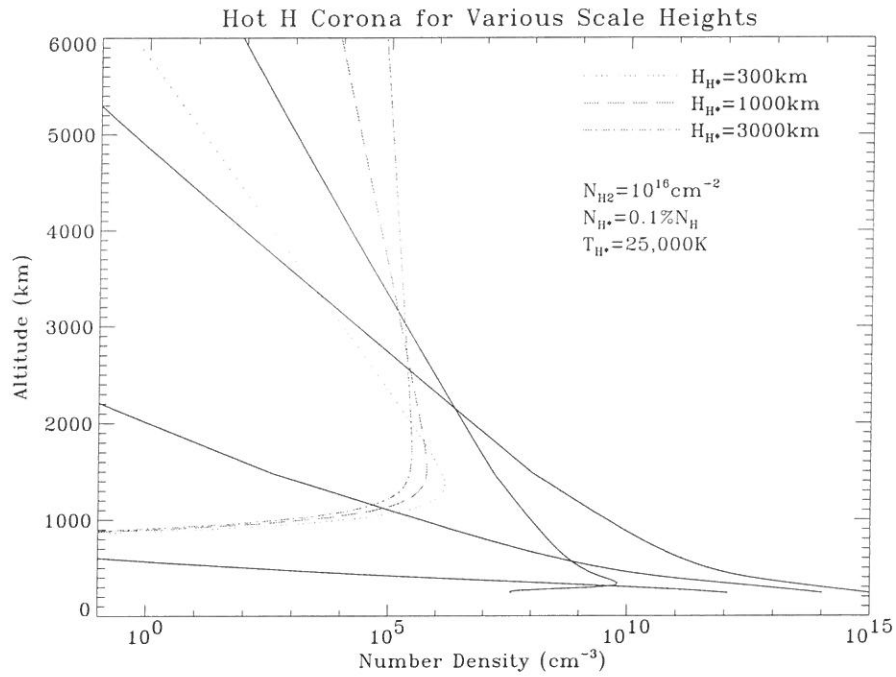


Fig. 8. Hot H profiles used for a study of the sensitivity of the model to variations in the hot H scale height. The remaining hot H parameters are held at their nominal values.

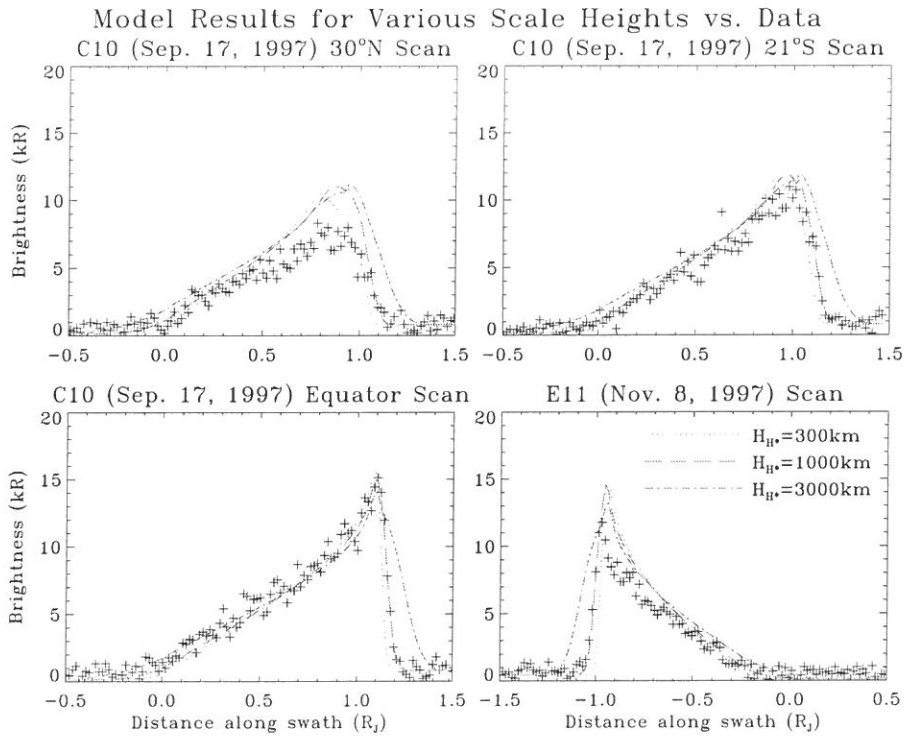


Fig. 9. The results of varying the hot H scale height on the model brightnesses. A factor of three in either direction away from the nominal scale height of 1000 km provide much worse fits to the data.

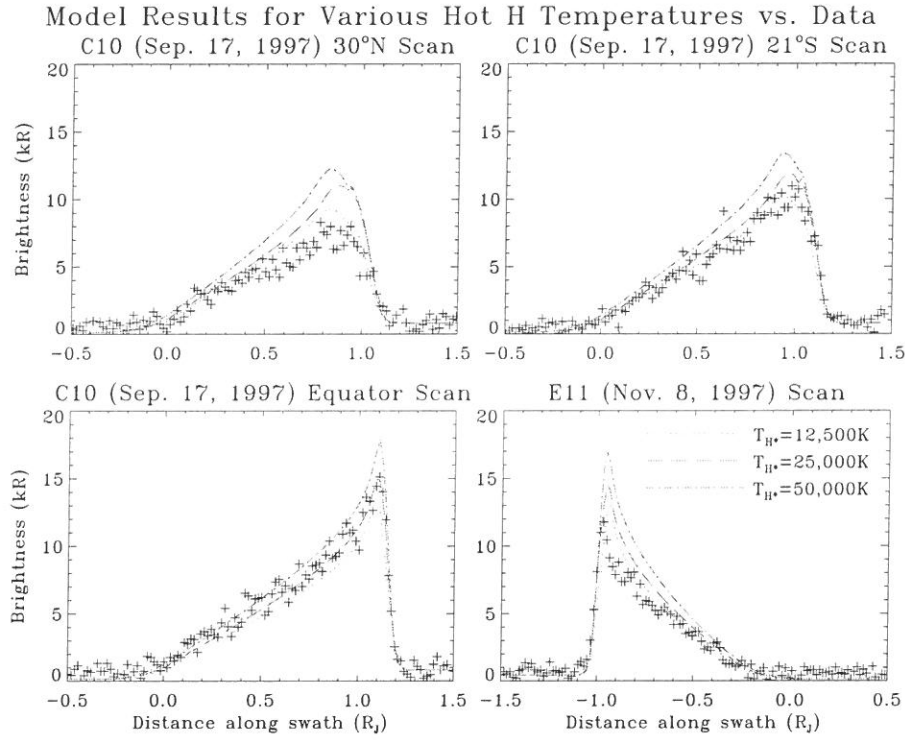


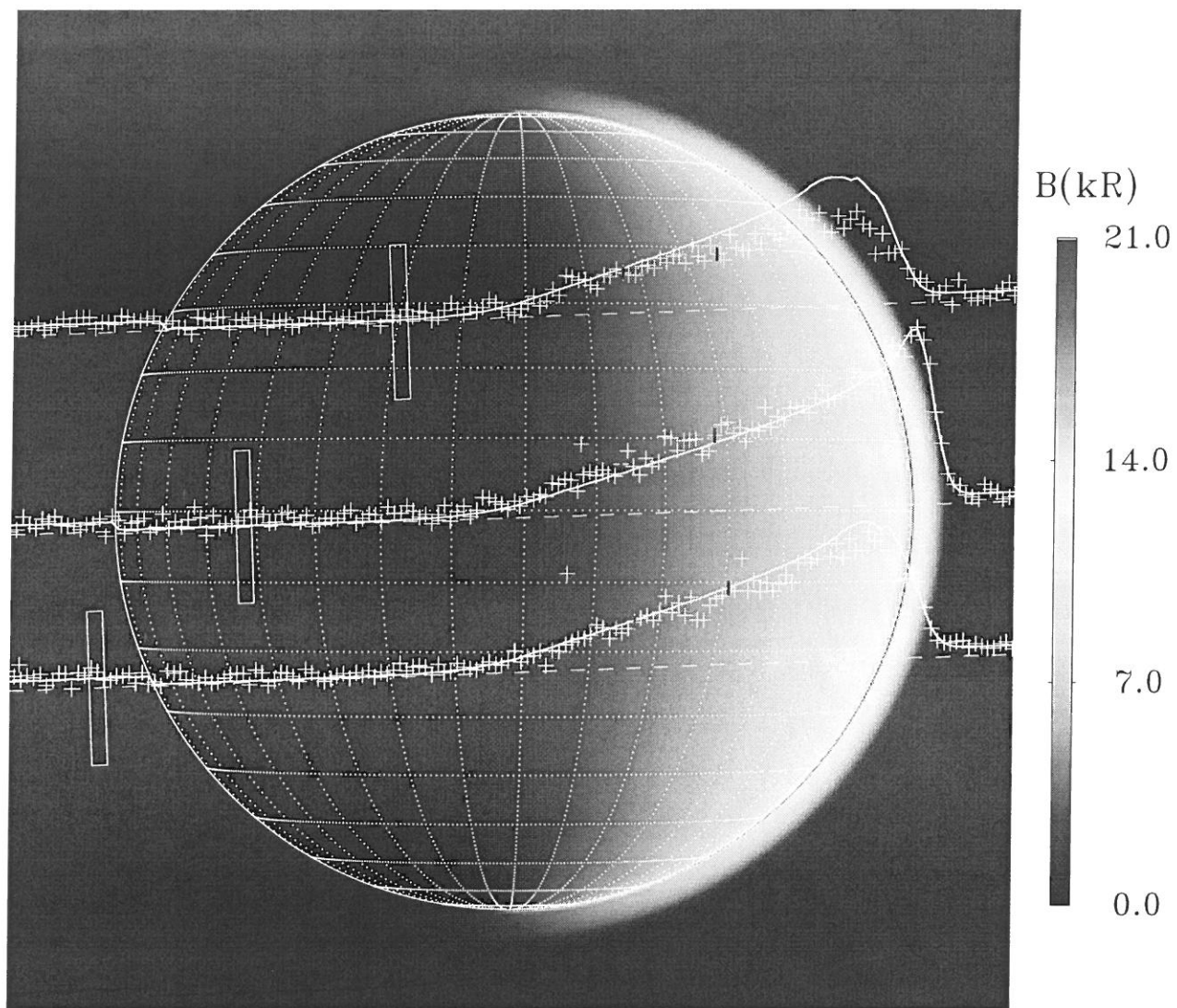
Fig. 10. The results of varying the effective hot H temperature on the model brightnesses. It is likely that a variety of combinations of effective hot H temperature and column density could be found that would fit the data equally well.

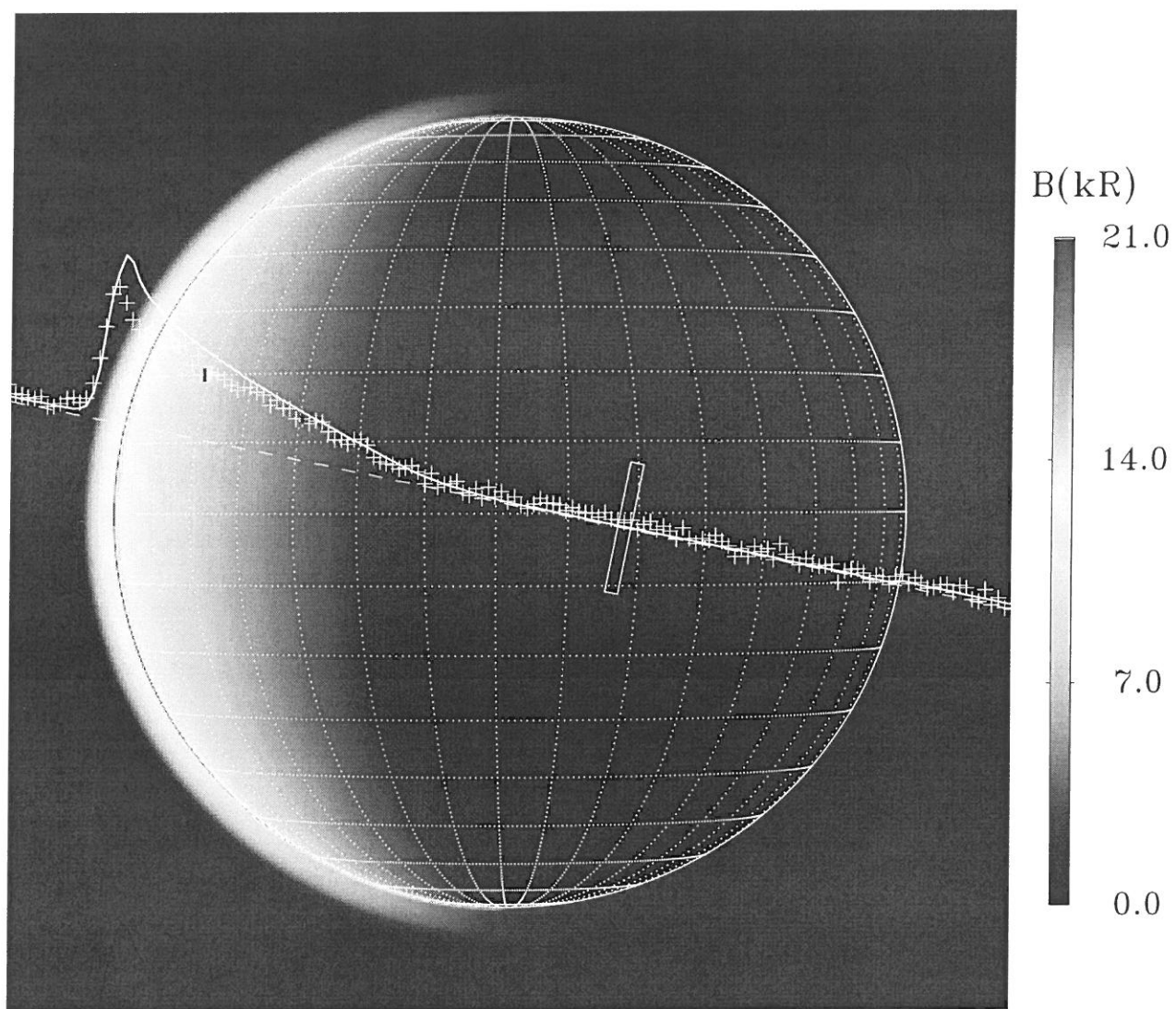
an empirically-based hot H model.

## References

- Ben Jaffel, L., Clarke, J.T., Prangé, R., Gladstone, G.R., Vidal-Madjar, A., 1993. The Lyman alpha bulge of Jupiter: Effects of non-thermal velocity field. *Geophys. Res. Lett.* 20, 747–750.
- Bisikalo, D.V., Shematovich, V.I., Gérard, J.-C., Gladstone, G.R., Waite, J.H., Jr., 1996. The distribution of hot hydrogen atoms produced by electron and proton precipitation in the Jovian aurora. *J. Geophys. Res.* 101, 21,157–21,168.
- Emerich, C., Ben Jaffel, L., Clarke, J.T., Prangé, R., Gladstone, G.R., Somneria, J., Ballester, G., 1996. Evidence for supersonic turbulence in the upper atmosphere of Jupiter. *Science* 273, 1085–1087.
- Gladstone, G.R., 1988. UV resonance line dayglow emissions on Earth and Jupiter. *J. Geophys. Res.* 93, 14,623–14,630.
- Gladstone, G.R., Allen, M., Yung, Y.L., 1996. Hydrocarbon photochemistry in the upper atmosphere of Jupiter. *Icarus* 119, 1–52.
- Gladstone, G.R., Yelle, R.V., Majeed, T., 2002. Solar system upper at-

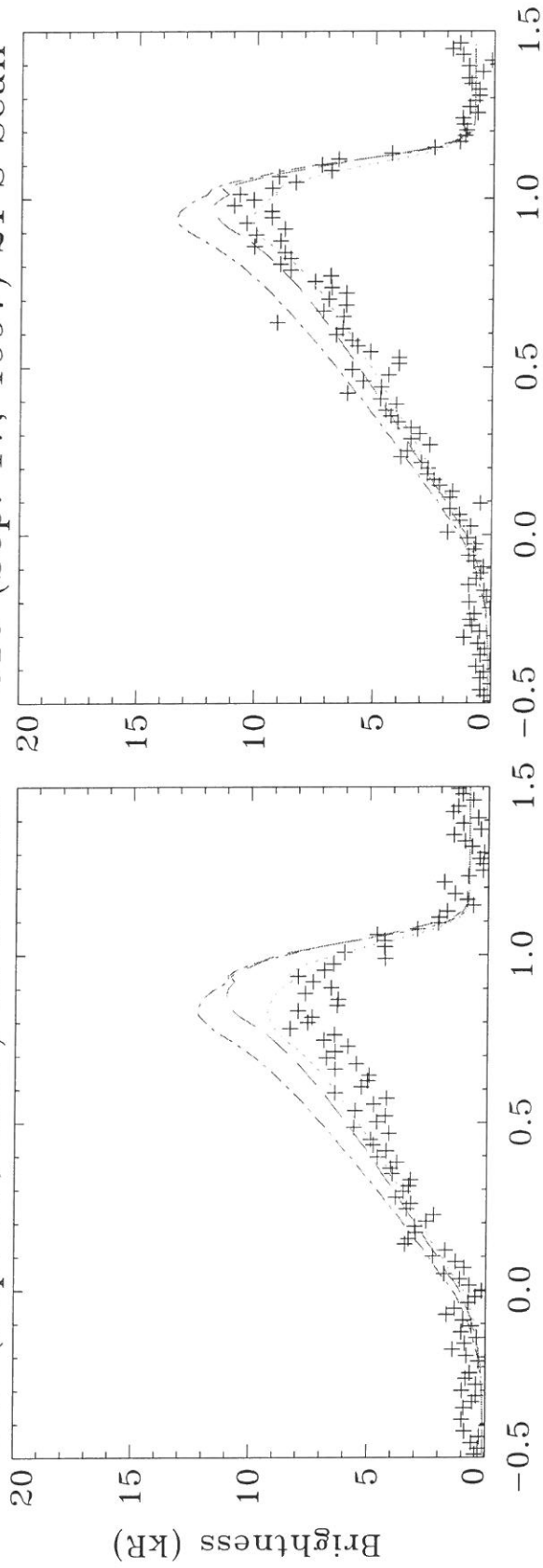
- mospheres: Photochemistry, energetics, and dynamics. In: Mendillo, M., Nagy, A., Waite, J.H. (Eds.), *Atmospheres in the Solar System: Comparative Aeronomy*. Geophysical Monograph 130, American Geophysical Union, Washington DC, pp. 23–37.
- Hord, C.W., McClintock, W.E., Stewart, A.I.F., Barth, C.A., Esposito, L.W., Thomas, G.E., Sandel, B.R., Hunten, D.M., Broadfoot, A.L., Shemansky, D.E., Ajello, J.M., Lane, A.L., West, R.A., 1992. Galileo ultraviolet spectrometer experiment. *Space Sci. Rev.* 60, 503–530.
- McConnell, J.C., Sandel, B.R., Broadfoot, A.L., 1980. Airglow from Jupiter's nightside and crescent: Ultraviolet Spectrometer observations from Voyager 2. *Icarus* 43, 128–142.
- Pryor, W.R., Stewart, A.I.F., Simmons, K.E., Witte, M., Ajello, J.M., Tobiska, W.K., Hall, D.T., 2001. Remote sensing of H from Ulysses and Galileo. *Space Sci. Rev.* 97, 393–399.
- Seiff, A., Kirk, D.B., Knight, T.C.D., Young, R.E., Mihalov, J.D., Young, L.A., Milos, F.S., Schubert, G., Blanchard, R.C., Atkinson, D., 1998. Thermal structure of Jupiter's atmosphere near the edge of a 5- $\mu$ m hot spot in the north equatorial belt. *J. Geophys. Res.* 103, 22,857–22,889.



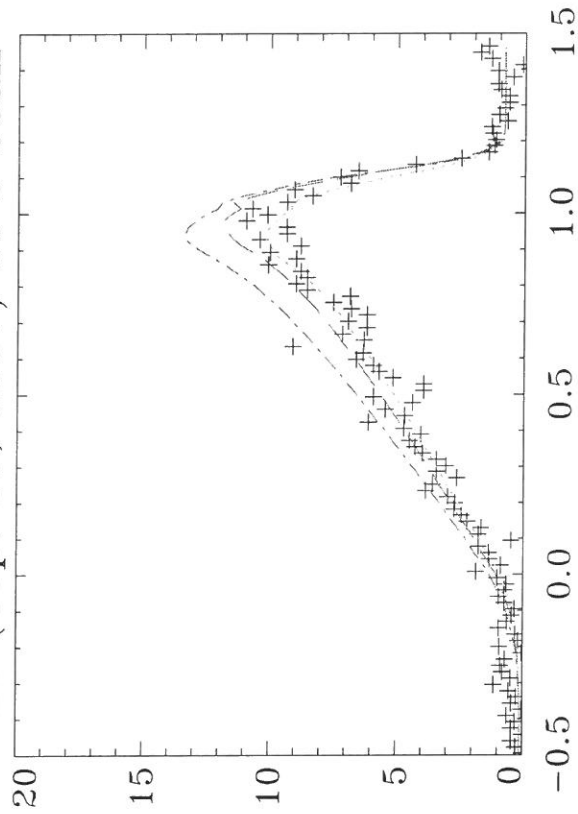


# Model Results for Various Hot H Temperatures vs. Data

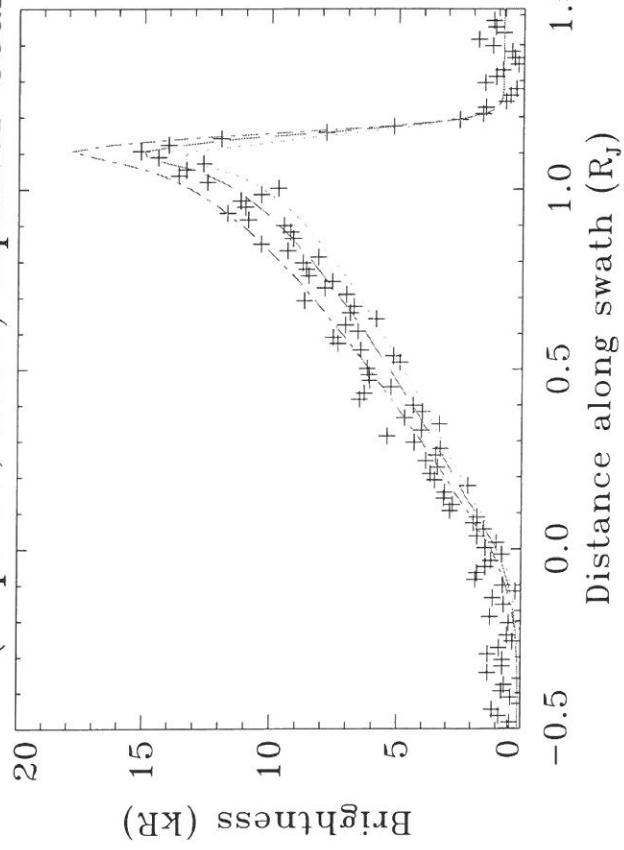
C10 (Sep. 17, 1997) 30°N Scan



C10 (Sep. 17, 1997) 21°S Scan



C10 (Sep. 17, 1997) Equator Scan



E11 (Nov. 8, 1997) Scan

